SUAS-Integrated Infrared Thermography for Rapid Thermal Mapping and Heat Transfer Evaluation

Ahmad Anas Yusof*, Dharshini Subramaniam

Department of Mechatronics Engineering, Faculty of Electrical Technology and Engineering, Universiti Teknikal Malaysia Melaka, Malaysia

***Corresponding Author**

DOI: https://doi.org/10.51244/IJRSI.2025.12120118

Received: 28 December 2025; Accepted: 03 January 2026; Published: 16 January 2026

ABSTRACT

This study investigates the use of small unmanned aerial systems (SUAS) integrated with infrared thermography for rapid thermal mapping and quantitative heat transfer evaluation in building environments. Thermal data are captured from various structural and surface elements under real outdoor conditions, enabling both conductive and radiative heat analyses. Conductive heat transfer is evaluated on high-density concrete elements, designated as a shaded wall, a shaded balcony, and an exposed balcony, using paired surface and interior temperature measurements in conjunction with Fourier's Law. The shaded balcony exhibits the highest heat transfer rate at 376 W, followed by the exposed balcony at 202.7 W, and the shaded wall at 164 W. For radiative heat transfer, analysis based on the Stefan–Boltzmann Law shows that a vegetative surface emits only 18.9 W, while a paved roadway emits a significantly higher 112.3 W, demonstrating the thermal buffering capacity of vegetation. These results confirm that SUAS-integrated thermal imaging provides a fast, scalable, and non-invasive method for identifying heat losses, detecting thermal inefficiencies, and informing energy-efficient urban and building design strategies.

Keywords: Infrared Thermography, Heat Transfer Analysis, SUAS Thermal Mapping

INTRODUCTION

The integration of small unmanned aerial systems (SUAS) with infrared thermography offers an advanced and efficient method for rapid surface temperature measurement on buildings and solar photovoltaic (PV) panels. This approach significantly contributes to smart energy management and real-time thermal monitoring and is spearheaded by the Robotics and Industrial Automation Research Group at the Faculty of Electrical Technology and Engineering.

Infrared thermography is a non-contact diagnostic technique that detects and measures infrared radiation emitted by surfaces, enabling the visualization and analysis of heat transfer patterns in building envelopes and energy systems. It is widely recognized as a valuable tool for preventive maintenance, fault detection, and performance optimization. By mounting thermal cameras on SUAS platforms, operators can access a wide range of viewpoints and altitudes, enhancing spatial coverage and measurement precision without the need for scaffolding or manual inspection.

This paper investigates the application of airborne infrared thermography using SUAS for rapid, remote temperature inspection of buildings and solar panels. The aim is to evaluate thermal behaviour, detect anomalies, and analyse factors affecting heat transfer performance. The study highlights the potential of drone-based thermographic systems as a scalable solution for sustainable building management and renewable energy monitoring.

The novelty of this study lies in the combined application of SUAS-based infrared thermography for both conductive and radiative heat transfer estimation within a single rapid field assessment framework. Unlike conventional thermographic inspections that focus primarily on qualitative anomaly detection, this work demonstrates a simplified yet practical approach for extracting quantitative heat transfer indicators from aerial thermal data, supporting fast thermal screening in urban building environments.

ISSN No. 2321-2705 | DOI: 10.51244/IJRSI |Volume XII Issue XII December 2025

LITERATURE REVIEW

This section reviews key literature on the use of infrared thermography for detecting thermal anomalies in buildings and PV systems, with an emphasis on studies that integrate small unmanned aerial systems (SUAS) to enhance spatial coverage, data acquisition speed, and safety. Furthermore, the theoretical foundations of conductive and radiative heat transfer are outlined to contextualize the analytical methods employed in this study, providing a framework for interpreting thermal data collected through SUAS-integrated infrared imaging.

Previous Studies on Infrared Thermography in Buildings and PV Panels

Infrared thermography (IRT) is widely recognized as a non-destructive diagnostic tool for evaluating building envelopes, enabling the detection of thermal bridges, air leakage, and moisture intrusion (Balaras and Argiriou, 2002). In the context of photovoltaic (PV) systems, IRT is commonly used to detect malfunctioning cells and hotspot development, which can significantly impact system performance (de Oliveira et al., 2022). However, traditional thermographic methods are often constrained by limited spatial coverage and manual data collection processes.

The integration of IRT with small unmanned aerial systems (SUAS) addresses these limitations by enabling rapid, high-resolution thermal assessments over complex structures and large areas. Mirzabeigi et al. (2025) demonstrated that aerial thermography provides broader and more consistent coverage of building envelopes compared to ground-based inspections. In the PV domain, Puppala et al. (2024) showed that SUAS-based thermographic inspections enhance the speed and accuracy of identifying thermal non-uniformities. Albatici et al. (2015) proposed a comprehensive validation framework for quantitative IRT in field inspections, confirming its utility for energy audits and retrofit planning.

Further advancements are seen in the integration of SUAS and artificial intelligence for scalable infrastructure diagnostics in complex or hazardous environments (Shrestha et al., 2025). Recent studies have extended these capabilities to real-world scenarios. One investigation demonstrated the effectiveness of SUAS-integrated IRT for rapid temperature measurement on building and PV surfaces, revealing surface temperatures ranging from 16.9°C to 63.8°C and emphasizing the importance of emissivity, reflectivity, and environmental context in interpreting thermal data (Yusof et al., 2024).

In agricultural settings, thermal and RGB drone imagery was used to monitor land preparation and vegetation thermal response in a durian orchard, illustrating how thermal gradients relate to soil–plant conditions (Yusof et al., 2022). Another study employed NDVI and RGB imaging from SUAS platforms for monitoring campus vegetation health and surface temperature variation, supporting their relevance in environmental management applications (Yusof et al., 2023). Together, these works underscore the growing role of SUAS-integrated thermography and multispectral imaging in enabling rapid, scalable, and data-rich diagnostics across diverse domains, including energy, agriculture, and environmental monitoring.

Governing Equations for Heat Transfer Evaluation

Heat transfer through building envelopes or PV modules is governed by conduction, convection, and radiation principles. For thermographic interpretation, conduction is often the dominant mode, especially in solid materials like walls, roofs, and solar panel layers. However, radiative heat transfer also plays a crucial role, particularly in surface-level interactions influenced by material properties. Materials with high emittance absorb and radiate more energy, which significantly affects thermal behaviour in buildings. Conversely, low-emittance materials reflect more radiation and emit less heat. Infrared thermography detects this emitted radiation and converts it into visual images that represent surface temperature. The primary governing equation used in this study is Fourier's Law of Heat Conduction:

$$\dot{Q} = kA\,(T_o - T_i) \tag{1}$$

where $\dot{Q}$ represents the conductive heat transfer in watts (W), k is the thermal conductivity of the material (W/m·K), A is the surface area in square meters (m²), and T_o and T_i are the outdoor and indoor surface temperatures in Kelvin (K).

For radiative heat transfer, particularly relevant in surfaces and plants, the Stefan-Boltzmann's Law may also be applied:

$$Q = \epsilon\sigma A(T_s^4 - T_a^4) \tag{2}$$

ISSN No. 2321-2705 | DOI: 10.51244/IJRSI |Volume XII Issue XII December 2025

where $\dot{Q}$ represents the radiative heat transfer in watts (W), ϵ is the emissivity of the surface, σ is the StefanBoltzmann constant (5.67×10^{-8} W/m²K⁴), A is the surface area in square meters (m²), and T_s and T_a are the surface and ambient temperatures in Kelvin (K). In combination with IR camera data and surface emissivity values, these equations allow for an accurate estimation of heat loss or gain, offering quantitative insights into the effectiveness of insulation and PV system performance. The reviewed literature establishes a strong foundation for integrating SUAS and IRT technologies in built environment diagnostics and solar energy monitoring. However, standardization of flight protocols, calibration methods, and environmental corrections remains a critical area for further investigation.

For the purpose of this study, several simplifying assumptions were adopted to enable rapid, field-based heat transfer estimation using SUAS-acquired thermal data. Heat conduction was assumed to be one-dimensional and steady-state, with uniform material properties and negligible thermal contact resistance. Convective heat transfer at the surface was not explicitly modelled, as the focus was on relative conductive heat flux comparisons between elements under similar environmental conditions. For radiative heat transfer calculations, a unit view factor was assumed, and surrounding surface radiation was neglected, resulting in simplified radiative emission estimates rather than a full radiative exchange model. These assumptions introduce uncertainty but are considered acceptable for comparative analysis and rapid thermal screening applications.

METHODOLOGY

This section outlines the methodological framework used to conduct rapid thermal mapping for heat transfer evaluation. A structured approach was adopted, including careful site selection, standardized drone configuration, precise data acquisition timing, and thorough image processing. The integration of SUAS and infrared thermography required attention to both technical specifications and environmental variables to ensure reliable and reproducible thermal results.

Study Area and Assets

The study was conducted within an urban academic setting at Universiti Teknikal Malaysia Melaka (UTeM), Malaysia. Specifically, the focus area was limited to the main lobby of the Faculty of Electrical Technology and Engineering, selected due to its accessibility, architectural exposure, and prior thermal inspection relevance. This location features mixed-use building characteristics providing a representative environment for evaluating surface heat transfer using SUAS-integrated infrared thermography (Fig. 1 and 2).

Thermal surveys are conducted in the afternoon (approximately 3:00 PM) to capture peak surface temperatures and maximize thermal contrast between sun-exposed and shaded areas. Ambient conditions, including temperature, humidity, and solar irradiance are recorded using the Parrot Bebop-Pro Thermal drone, which integrates both visual and thermal imaging sensors. This setup enables synchronized collection of environmental and surface temperature data, supporting accurate thermal analysis across different building materials and exposure conditions.

Indoor surface temperatures were obtained using a handheld digital thermometer positioned on the interior side of the corresponding wall or balcony element at the time of aerial thermal inspection to ensure temporal consistency between indoor and outdoor measurements.

Fig. 1 Main lobby of the Faculty of Electrical Technology and Engineering (From above)

ISSN No. 2321-2705 | DOI: 10.51244/IJRSI |Volume XII Issue XII December 2025

Fig. 2 Main lobby of the Faculty of Electrical Technology and Engineering (From oblique angle)

SUAS Configuration, Data Processing and Analysis

A Parrot Bebop-Pro thermal drone equipped with a high-sensitivity thermal camera captures images and videos, enabling the creation of thermal maps for heat transfer analysis. The figure presents the technical specifications of a quadcopter drone used for aerial data collection. The drone weighs 604 grams and offers a maximum flight time of 25 minutes, powered by a 3350 mAh (38.19 Wh) Lithium-Ion Polymer battery. It supports GPS and GLONASS satellite systems for precise positioning and navigation.

Drone Performance	
Weight	604 g
Maximum Flight Time	25 Minutes
Battery Capacity	3350 mAh / 38.19 Wh
Battery Chemistry	Lithium-Ion Polymer
Flight Control System	
GNSS Support	GPS, GLONASS
Remote Controller / Transmitter	
Operating Frequency	2.4 GHz
Maximum Operating Distance	2 km at 2.4 G
Battery Chemistry	Lithium-Ion Polymer
Battery Capacity	2700 mAh
Camera	
Sensor	1/2.3" CMOS
Effective Pixels	14 MP

Fig. 3 Drone Specifications and Performance

The drone operates with a remote controller using a 2.4 GHz frequency, allowing a maximum control range of up to 2 kilometers. The remote controller itself is powered by a 2700 mAh Lithium-Ion Polymer battery. For imaging purposes, the drone is equipped with a 1/2.3-inch CMOS sensor camera that delivers 14-megapixel resolution, suitable for high-quality aerial photography and thermal or visual inspection tasks. The accompanying diagram (Fig. 3) shows the drone's top-down and perspective views, confirming a standard fourrotor configuration.

ISSN No. 2321-2705 | DOI: 10.51244/IJRSI |Volume XII Issue XII December 2025

The thermal camera onboard the Parrot Bebop-Pro was configured using manufacturer-recommended settings, with emissivity values assigned based on standard material references. Surface temperature measurements were obtained under stable weather conditions to minimize atmospheric interference. While the thermal sensor provides sufficient sensitivity for relative temperature mapping, the measurements are subject to inherent uncertainties related to sensor accuracy, viewing angle, surface emissivity variation, and distance to target. Consequently, the thermal data were primarily used for comparative heat transfer assessment rather than absolute energy quantification.

The captured imagery was subsequently processed and analysed using FreeFlight Thermal software, which enabled precise temperature mapping, comparative surface analysis, and integration of environmental parameters such as ambient temperature, humidity, and solar irradiance for contextual interpretation. Surface temperatures were calibrated using known emissivity values. Hotspot detection and temperature gradient analysis were performed using threshold segmentation and heat flux calculations based on Fourier's Law.

RESULT AND DISCUSSION

The heat transfer analysis revealed distinct differences in thermal behaviour between conductive building elements and radiative surfaces in the urban landscape. Surface temperature measurements taken at a 45° observation angle ranged from 31.3°C to 57.2°C (Fig. 4). Among the surfaces analysed, the sun-exposed balcony recorded the highest temperature at 53.2°C, followed closely by the roadway surface at 50.6°C. In contrast, shaded vertical walls measured 34.3°C, while shaded balconies registered a lower temperature of 37.2°C. The temperature of exposed plant surfaces was measured at 36.1°C.

It should be noted that surface temperature readings derived from infrared thermography may vary within a small range due to emissivity uncertainty, viewing angle, and local airflow conditions; however, these variations do not affect the comparative trends observed across the analysed surfaces.

To investigate heat transfer behaviour across different urban materials, both conductive and radiative heat transfer modes were examined. For conductive analysis, temperature readings were taken from three structural elements constructed using high-density concrete, with a known thermal conductivity, k, of 2.0 W/m·K and a uniform thickness of 0.15 m. These elements included a shaded wall, a shaded balcony, and an exposed balcony.

These findings clearly demonstrate the impact of solar exposure, with shading contributing to a significant reduction in surface temperature, for example, a temperature difference of 16°C was observed between the exposed (53.2°C) and shaded (37.2°C) balcony surfaces. This variation in surface temperature directly influences conductive and radiative heat transfer behaviour across building elements, prompting further analysis of selected concrete surfaces. The results of the heat transfer can be observed in Table 1 and 2.

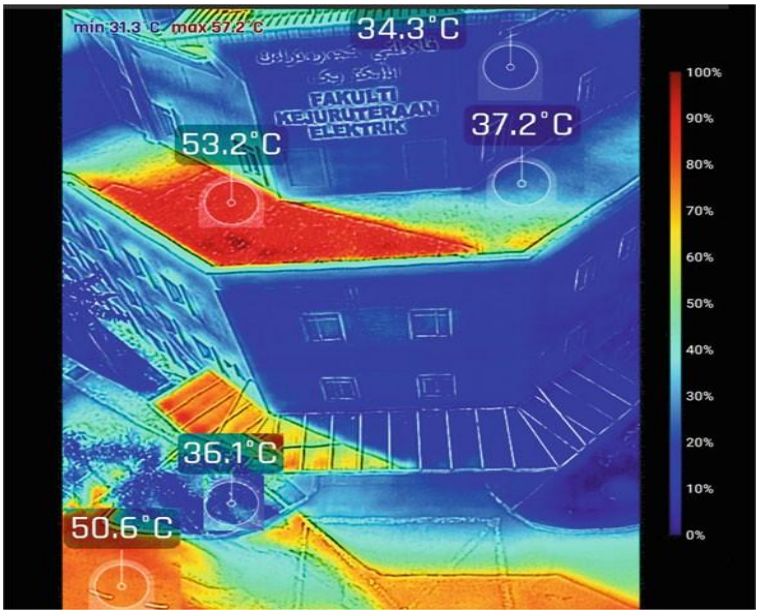

Fig. 4 Rapid Temperature Readings

ISSN No. 2321-2705 | DOI: 10.51244/IJRSI |Volume XII Issue XII December 2025

Conductive Heat Transfer

For conductive heat transfer, three concrete-based structural elements were evaluated: a shaded wall, a shaded balcony, and an exposed balcony. Using Fourier's Law and assuming a uniform surface area of 1 m², the shaded wall, with a surface temperature of 34.3°C and an interior temperature of 22°C, showed a heat transfer rate of 164 W. The shaded balcony, which recorded the highest surface temperature among the conductive samples (53.2°C), and an interior temperature of 25°C, had the highest heat transfer rate at 376 W. Meanwhile, the exposed balcony showed a surface temperature of 37.2°C and an interior of 22°C, corresponding to a moderate heat transfer of 202.7 W. These results indicate that solar exposure and surface temperature strongly influence conductive heat gain, even when the structural materials and thickness remain constant. The significant heat flow through the shaded balcony suggests potential heat accumulation or delayed cooling due to limited ventilation or retained heat from prior exposure. Conversely, the shaded wall, having the lowest temperature gradient, resulted in the least conductive heat gain, emphasizing the importance of shading in minimizing building heat load.

Table 1: Conductive Heat Transfer Results

Element	Outdoor Surface Temperature (°C)	Indoor Surface Temperature (°C)	Material	Thermal Conductivity k (W/m·K)	Thickness (m)	Notes	Heat Transfer (W)
Wall (Shaded)	34.3	22	Highdensity concrete	2.0	0.15	Shaded wall	164
Balcony (Shaded)	53.2	25	Highdensity concrete	2.0	0.15	Shaded balcony	376
Balcony (Exposed)	37.2	22	Highdensity concrete	2.0	0.15	Exposed balcony	202.7

It should be noted that the higher conductive heat transfer observed in the shaded balcony, despite its classification as shaded, may be influenced by residual heat storage within the concrete mass and reduced convective cooling due to limited airflow. This suggests that transient thermal effects and structural geometry can significantly affect heat transfer behaviour, even in the absence of direct solar exposure.

Radiative Heat Transfer

For radiative heat transfer, the plant surface (36.1°C) and roadway surface (50.6°C) were compared to an ambient temperature of 33°C using the Stefan–Boltzmann Law. The plant, with an assumed emissivity of 0.95, emitted approximately 18.9 W of radiative heat, while the roadway, with an emissivity of 0.90, emitted a significantly higher 112.3 W. This contrast underscores the thermal buffering role of vegetation, which emits far less heat back to the environment than hardscape materials like asphalt. Such findings support the integration of green infrastructure to mitigate urban heat effects, reduce surface temperatures, and enhance thermal comfort. Overall, the results demonstrate that material type, exposure condition, and thermal properties play critical roles in urban heat dynamics. Concrete structures, though similar in composition, exhibited large variations in heat transfer due to orientation and solar gain, while vegetative and paved surfaces differed widely in radiative emission despite experiencing similar ambient conditions.

Table 2: Radiative Heat Transfer Results

Element	Outdoor Surface Temperature (°C)	Ambient Temperature (°C)	Emissivity (ε)	Notes	Heat Transfer (W)
Plant	36.1	33	0.95	Vegetation/leaf	18.9
Roadway	50.6	33	0.9	Asphalt/concrete road	112.3

The calculated radiative heat values represent simplified emission estimates and are intended to illustrate relative thermal behaviour between vegetated and hardscape surfaces rather than precise net radiative heat exchange with the environment.

CONCLUSION

This study shows that SUAS-integrated infrared thermography can effectively detect and analyse heat patterns on buildings and nearby surfaces in real conditions. Heat transfer through concrete was found to vary with sunlight exposure: the shaded balcony had the highest rate at 376 W, followed by the exposed balcony at 202.7 W, and the shaded wall at 164 W. This highlights how solar exposure affects heat gain, even when the material is the same. For radiative heat transfer, vegetation released only 18.9 W, while hard surfaces like roads emitted up to 112.3 W, showing the cooling benefit of green areas. The findings indicate that SUAS-integrated thermography can support early-stage energy audits, identification of thermally inefficient building components, and evaluation of urban surface materials with minimal disruption and time investment. While the presented heat transfer values are simplified, they provide actionable insights for comparative assessment, enabling engineers and planners to prioritize detailed investigations and mitigation strategies. Overall, the method offers a quick, scalable, and non-invasive way to gather important thermal data for improving energy efficiency and climateadaptive building design.

REFERENCES

1. Balaras, C.A., Argiriou, A.A. (2002). Infrared thermography for building diagnostics. Energy and Buildings 34(2), 171–183. https://doi.org/10.1016/S0378-7788(01)00105-0
2. de Oliveira, A. K. V., Aghaei, M., & Rüther, R. (2022). Automatic Inspection of Photovoltaic Power Plants Using Aerial Infrared Thermography: A Review. Energies, 15(6), 2055. https://doi.org/10.3390/en15062055
3. Mirzabeigi, S., Razkenari, R., & Crovella, P. (2025). A review of the potential of drone-based approaches for integrated building envelope assessment. Buildings, 15(13), 2230. https://doi.org/10.3390/buildings15132230
4. Puppala, H., Maganti, L. S., Peddinti, P. R., & Motapothula, M. R. (2024). Thermographic inspections of solar photovoltaic plants in India using Unmanned Aerial Vehicles: Analysing the gap between theory and practice. Renewable Energy, 237, 121694. https://doi.org/10.1016/j.renene.2024.121694
5. Albatici, R., Tonelli, A.M., & Chiogna, M. (2015). A comprehensive experimental approach for the validation of quantitative infrared thermography in the evaluation of building thermal transmittance. Applied Energy 141, 218–228. https://doi.org/10.1016/j.apenergy.2014.12.035
6. Shrestha, P., Avci, O., Rifai, S., Abla, F., Seek, M., Barth, K., & Halabe, U. (2025). A review of infrared thermography applications for civil infrastructure. Structural Durability and Health Monitoring,19(2),193-231. https://doi.org/10.32604/sdhm.2024.049530
7. Yusof, A.A., Yahya, M.F., Miskon, M.F., Nor, M.K.M., Kasim, A.M., Jamri, M.S., & Rizal,N.S.M. (2024). SUAS-Based Infrared Thermography for Rapid Temperature Measurement in Building and Solar Photovoltaic Panels for Thermal Distribution Analysis. In: Hamidon, R., Bahari, M.S., Sah, J.M., Zainal Abidin, Z. (eds.), Lecture Notes in Mechanical Engineering, Intelligent Manufacturing and Mechatronics, pp. 257–270. Springer, Singapore. https://doi.org/10.1007/978-981-97-0169-8_19
8. Yusof, A.A., Nor, M.K.M., Mohd Shaari, N.L.A., Kassim, A.M., Shamsudin, S.A., Sulaiman, H., & Hanafi, M.A. (2022). Land clearing, preparation and drone monitoring using RGB and thermal imagery for smart durian orchard management. Journal of Advanced Research in Fluid Mechanics and Thermal Sciences 91(1), 115–128. https://doi.org/10.37934/arfmts.91.1.115128
9. Yusof, A.A., Yahya, M.F., Nor, M.K.M., & Miskon, M.F. (2023). SUAS-based NDVI and RGB image for remote landscape and environmental monitoring on university campus. In: Abdullah, M.A. et al. (eds.), Advances in Intelligent Manufacturing and Mechatronics, Lecture Notes in Electrical Engineering, vol. 988, pp. 251–261. Springer, Singapore. https://doi.org/10.1007/978-981-19-8703-8_21